

Experimental Analyses of the Retinal and Subretinal Haemorrhages Accompanied by Shaken Baby Syndrome / Abusive Head Trauma Using a Dummy Doll

Junpei Yamazaki^{a,1}, Makoto Yoshida^{a,2,*}, Hiroshi Mizunuma^a

^a*Department of Mechanical Engineering, Tokyo Metropolitan University, 1-1 Minami-Osawa, Hachioji, Tokyo 192-0397, Japan*

Abstract

Introduction: We explored several modes of violent shaking using a dummy doll with an eyeball model to reproduce abusive events that lead to retinal haemorrhages (RH) seen in shaken baby syndrome or abusive head trauma (SBS / AHT).

Materials and Methods: A dummy doll equipped with an eyeball model was prepared. The eyeball model was filled with a model of vitreous body, *i.e.* agar gel or water, and was with a pressure sensor to measure normal stress.

Results: The modes of shaking were classified into three patterns, *i.e.* fast shaking with the fore arms, fast shaking with the whole arms and synchronized shaking with the whole arms. The frequency of the cyclic acceleration-deceleration history experienced by the head of the dummy doll was 5.0, 4.0 and 2.2 Hz, respectively, with the maximum acceleration of 20, 20 and 60 m/s², respectively. We considered the last of these three modes of shaking as possibly corresponding to the worst case of violent shaking. This mode of shaking could be instructed to volunteers who acted as imitate perpetrators, and resulted in both increased peak intensities of the acceleration experienced by the head of the dummy doll and increased stresses on the retina at the posterior pole of the eyeball model.

Discussion: The time integral of the stress through a single cycle of shaking was 107 Pa·s, much larger than that of a single event of fall, which resulted in 60 to 73 Pa·s. Taking into account that abusive shaking is likely to include multiple cycles, the time integral of the stress due to abusive shaking can be even larger. This clear difference may explain why RH in SBS / AHT is frequent, while RH in accidental falls is rare.

Keywords: Shaken baby syndrome, Abusive head trauma, Retinal haemorrhage, Stress, Vitreous body

*Corresponding author

Email addresses: junpei_yamazaki@tte-net.co.jp (Junpei Yamazaki), yoshida-makoto@tmu.ac.jp (Makoto Yoshida), mizunuma@tmu.ac.jp (Hiroshi Mizunuma)

¹Present address: Takasago Thermal Engineering Co., Ltd., 4-2-5 Kanda-Surugadai, Chiyoda, Tokyo 101-8321, Japan

²telephone: +81-42-677-1111, facsimile: +81-42-677-2701

1. Introduction

Shaken baby syndrome or abusive head trauma (SBS / AHT) is a series of abusive head injuries caused by abusive shaking. Some of the characteristic findings in SBS / AHT are subdural haemorrhages, cerebral contusion and extensive retinal haemorrhages (RH)^{1,2}. The diagnosis of SBS / AHT can be difficult because external bruising, which can be a stark evidence, has been reported to be absent in a significant minority (21%) of fatal abusive head injuries³. Although the mechanism of RH on abusive shaking is not clearly understood, pediatric ophthalmologists examine the fundus of children suspected to having been abused because RH is found in 83% of the shaken children⁴. RHs caused by SBS / AHT are often bilateral, involve the preretinal layer, cover the macula and extend to the periphery of the retina; while those due to accidental impacts are usually unilateral, accompanied by scalp haematoma, restricted to cases that cause severe epidural haematoma^{5,6}. While differential diagnosis of SBS / AHT are carefully made with the aid of these characteristic tendencies, that accidental falls also could cause RH might still be used as an excuse by a perpetrator. Therefore, elucidation of the mechanism of RH in SBS / AHT can be very helpful for rational identification of child abuse.

The diameter of an eyeball is *ca.* 24 mm in adults and *ca.* 16 mm in newborns. The outermost layer of an eyeball consists of the cornea and the sclera, which maintain the spherical shape of the eyeball. The cornea is a transparent membrane located in the anterior surface to lead light into the eyeball, whose area occupies 1/5 of the surface of the eyeball. The sclera is a white opaque and strong membrane that occupies the rest 4/5 of the surface of the eyeball. The retina, the tissue that senses light, is a thin and soft membrane located inside the eyeball. The vitreous body is a transparent tissue that occupies about 2/3 of the volume of the eyeball. The ingredient of gel of the vitreous body decreases along aging⁷.

Duhaime et al.⁸ estimated the acceleration experienced by the head of an infant during abusive shaking, using a dummy doll equipped with an accelerometer. Their simulated abusive shaking had a frequency of *ca.* 4 Hz, according to commonly described situation of SBS / AHT. Nevertheless, the actual situation of abusive shaking may not be correctly described because of the scarceness of objective witness.

The hypothesis of vitreoretinal traction, which postulates that the stress applied on the retina drawn by the vitreous body during abusive shaking causes RH, is attracting attention as the major factor of RH in SBS / AHT⁹. Hans et al.¹⁰ and Rangarajan et al.¹¹ tried to verify this hypothesis by estimating the stress applied on the retina, using finite element method. However, both of these studies assumed some frequency and amplitude for the abusive shaking.

In this study, we attempt to analyze abusive shaking mechanically and to estimate the stress applied on the retina of the victims through experiments using a dummy doll equipped with an eyeball model, with some improvements with respect to the previous studies as follows. We explored some modes of shaking as an attempt to better reproduce abusive shaking, instead of assuming some fixed frequency and amplitude.

In addition, the eyeball model was with a pressure sensor to estimate the stress applied on the retina experimentally. These improvements make our study distinct from others^{8,10,11}.

2. Materials and Methods

2.1. Preparation of the eyeball model

An eyeball model was prepared to estimate the stress applied on the retina (Fig. 1A). The plastic casing of the eyeball model was made with a 3D printer (Dimension SST 1200es, Stratasys Ltd., Eden Prairie, MN, USA), the inside of which was a spherical void with a diameter of 20 mm. Either agar gel or water was filled as a model of the vitreous body. Hot solution of agar was carefully injected into the assembled casing with a syringe through a small opening located at the opposite side with respect to the location of the pressure sensor. Air bubbles were led out through the opening by frequently flicking the casing, and the opening was plugged afterwards. Every experimental setups, disassembled after the experiments, were confirmed to be free of air bubbles. A pressure sensor (PS-05KD, Kyowa Electronic Instruments Co., Ltd., Tokyo, Japan) with a diameter of 6 mm was placed on the inside wall of the casing to record the temporal stress change of the part of the model compared to the retina. The signal from the pressure sensor had been offset against the atmospheric pressure. The signal from the pressure sensor was inverted so could be considered as the total stress normal to the surface of the sensor, because 'compressive' pressure is defined as positive whereas compressive stress is defined as negative. The flat diaphragm surface of the pressure sensor, flush-mounted to the inner surface of the casing, inevitably causes deviation from spherical geometry. While the commercially available pressure sensor with the smallest area was chosen to minimize this problem, the diameter of the eyeball model still had to be set somewhat larger than that of infants (but smaller than that of adults) so as to prevent significant deviation.

The physical properties of the vitreous body is known to change from gel-like state to more liquefied state along aging—there are some evidence indicating some liquefied vitreous body in a four-year old child, and about one fifth of the vitreous body is liquefied in teenagers¹². Furthermore, *in vivo* measurements of elastic properties of vitreous body of human do not agree well with each other^{13,14,15}, indicating the difficulty of the measurement. Admitting that the use of agar gel enclosed in a plastic casing is already a rough approximation, we introduced surgical experience to determine *ad hoc* concentration of the agar gel to mimic the vitreous body of infants. Therefore, we performed a sensory evaluation to determine the Young's modulus of the vitreous body of infants, based on surgical experience of a pediatric ophthalmologist. We employed agar gel as a model material and the kinesthetic sense during suction through a syringe needle (27 gauge \times 3/4") was evaluated. Agar gels were prepared at the concentrations of 0.5, 0.6, 0.7, 0.8, 0.9 and 1.0%, which were immersed in glycerin to avoid air suction. Consequently, 0.5% agar was determined to be optimal to simulate the mechanical property of the vitreous body of infants. We also employed water and

1% agar gel as alternative models of the vitreous body to check the robustness of our measurement; if the measured stress is not too dependent on the model of the vitreous body, it would be rather reliable without precisely knowing the true elastic properties of the vitreous body.

Moduli of viscoelasticity of the agar gels were measured with a rotational rheometer (HAAKE RheoStress 600, Thermo Fisher Scientific Inc., Waltham, MA, USA). The storage modulus G' and the loss modulus G'' were measured by a frequency sweep at the shearing stress of 10 Pa. The agar gel subjected to the measurement was a cylinder with the diameter of 35 mm and the height of 4.3 mm. Young's moduli of the agar gels were measured with a compressive testing apparatus. The stress and the strain were measured at a compressive velocity of 10 mm/s. The agar gel subjected to the measurement was a cube with the sides of 16 mm. The volume of the agar gels subjected to these measurements were set close to that of the spherical void of the eyeball model.

2.2. Preparation of the dummy doll

A baby doll (CHOU CHOU, Zapf Creation AG, Rödental, Germany) equipped with the eyeball model was shook by an imitate perpetrator to obtain data of violent shaking and its effect on the fundus of the eyeball (Figs. 1B and C). This doll was also subjected to free falling. The mass of the doll, simulating an one-month-old infant, was controlled by stuffing with iron pellets and wet cotton; the mass of the head of the doll was set to 0.8 kg, and the whole mass of the doll was set to 4 kg⁸. The neck of the doll only tethered the head to the body, similarly to an infant.

2.3. Simulation of violent shaking using a dummy doll

An imitate perpetrator, with an accelerometer (AS-50B, Kyowa Electronic Instruments Co., Ltd., Tokyo, Japan) attached to either of his/her hands, held the dummy doll by the armpits face-to-face. Another accelerometer was set on the head of the dummy doll. The coordinate system of the simulated violent shaking is summarized in Fig. 1D. Moving pictures of the shaking events by an imitate perpetrator were taken at 100 frames per second with a high-speed camera (MEMRECAMci, nac Image Technology Inc., Tokyo, Japan).

2.4. Application of machine-controlled oscillation on the eyeball model

To investigate the stress in the eyeball model due to a shaking event in a reproductive fashion, one axis oscillation generated by an oscillation machine (mod.J076-171, Kayaba Industry Co., Ltd, Tokyo, Japan) was conducted. A sinusoidal shaking with a frequency of 5.0 Hz and an amplitude of 30 mm and a rectangular pulse movement with an amplitude of 60 mm were applied. The displacement of the eyeball model was measured with a laser sensor (ZX-LD100, OMRON Corporation, Kyoto, Japan).

3. Results

3.1. Characteristics of violent shaking

An imitate perpetrator shook the dummy doll in various ways, which were classified into three modes (Figs. 2-4). When the imitate perpetrator shook the dummy doll as fast as possible with the fore arms, the displacement of the head of the doll was minor (Fig. 2A). The movement of the head of the doll was also minor (Fig. 2B). The frequency of the shaking was *ca.* 5.0 Hz, and the acceleration experienced by the head of the doll was *ca.* 20 m/s², which was smaller than that recorded on the hand of the imitate perpetrator, *ca.* 40 m/s² (Fig. 2C). When the imitate perpetrator shook the dummy doll with the whole arms with large strokes, and as fast as possible, the head of the dummy doll moved with some rotational moment (Fig. 3A). The frequency of the shaking was *ca.* 4.0 Hz, and the acceleration experienced by the head of the doll was *ca.* 20 m/s², which was smaller than that recorded on the hand of the imitate perpetrator, *ca.* 60 m/s² (Fig. 3C). When the imitate perpetrator shook the dummy doll with the whole arms and synchronized the movement of the body of the doll with that of its head, the horizontal displacement of the eyeball model was maximal, exceeding 40 cm (Fig. 4B). The frequency of the shaking was *ca.* 2.2 Hz, and the acceleration experienced by the head of the doll exceeded *ca.* 60 m/s², which was comparable or larger than that recorded on the hand of the imitate perpetrator, 60 m/s² (Fig. 4C).

Duhaime et al.⁸ reported that maximal acceleration experienced by the head of an infant during abusive shaking as 136 m/s², 56 m/s² and 69 m/s², for models of infant with hinge neck, flexible rubber neck and stiff rubber neck, respectively. While the first one seems to be an overestimation, our values obtained with the dummy doll with tethered neck roughly agrees with the latter two. The shape of the trace of the acceleration reported in their study also roughly agreed with ours. Thus, we were able to further explore modes of shaking using an experimental setup comparable to a previous study.

Although the acceleration recorded on the hand of the imitate perpetrator was almost the same between the modes of shaking shown in Figs. 3 and 4, that experienced by the head of the doll was much larger in the latter, basically due to the resonant nature of the shake. The mode of shaking shown in Fig. 4 can be possibly the worst case of violent shaking.

Some female volunteers were asked to shake the dummy doll in order to investigate whether women, who have generally less physical strength than men, can really cause SBS / AHT. This is a question worthy of consideration, at least in Japan, because a literature¹⁶ pointed out two idiosyncratic features in Japanese SBS / AHT cases compared to the Western cases: 1. The mother is more frequently the perpetrator. 2. The abusive parents are older than those in the United States of America. Five Japanese women and one Japanese man (who explored the modes of shaking in Figs. 2-4) role-played a situation to stop an infant cry by shaking with emotional excitement. Table 1 shows the characteristics of the imitate perpetrators. Firstly, the imitate perpetrator shook the dummy doll in their own ways (Table 2), and then

were instructed to reproduce the mode of shaking shown in Fig. 4 (Table 3). The frequency of the cycle of acceleration-deceleration experienced by the head of the dummy doll has decreased from *ca.* 2.4 Hz to *ca.* 1.7 Hz by the instruction. The average of the peak intensities of the acceleration experienced by the head of the dummy doll and that of the stress at the posterior pole has increased after the instruction. The results implies that women are able to shake an infant as hard as a man can if they shake in the mode of shaking shown in Fig. 4. This mode of shaking seems to be a more important factor than physical strength to cause SBS / AHT.

3.2. Agar as the model material of the vitreous body

As a result of sensory evaluation based on surgical experience, the optimal concentration of agar gel as a model of an infant vitreous body was determined to be 0.5%. Figs. 5A and 5B show the viscoelasticity of 1.0% and 0.5% agar gels, respectively. Agar gels in this concentration range can be regarded as elastic bodies because G'' was negligible compared to G' . A recent *in vivo* viscoelasticity measurement reported that both G' and G'' of adult human vitreous body were 3 ± 1 hPa (0.3 ± 0.1 kPa)¹⁵. That the order of magnitude of the G' agree with our value for 0.5% agar gel, *ca.* 0.7 kPa (Fig. 5B), partly supports the validity of our primitive model. Figs. 5C and 5D show the stress-strain curves of compressive tests of 1.0% and 0.5% agar gels, respectively. The Young's moduli E of 0.5% and 1.0% agar gels were determined to be *ca.* 1.9 kPa and *ca.* 30.3 kPa, respectively, from the gradient of the graphs. Nevertheless, the change of the model of the vitreous body did not have a prominent effect on the estimated stress experienced by the retina, as described in the following sections. Thus we were fortunately able to obtain reliable experimental estimate of the stress experienced by the retina.

3.3. Estimating the stress applied on the retina

Fig. 6 shows the stress during shaking event at the posterior pole of the eyeball model containing different materials as the model of the vitreous body. When the eyeball model contained 1.0% agar gel as the model of the vitreous body, the peak compressive stresses were 0.5-0.6 kPa and the peak tensile stresses were 1.0-1.4 kPa. When the eyeball model contained 0.5% agar gel as the model of the vitreous body, the peak compressive stresses were 0.6-0.7 kPa and the peak tensile stresses were 0.9-1.4 kPa. Both compressive and tensile stresses were almost proportional to the acceleration experienced by the head of the dummy doll. When the eyeball model contained water as the model of the vitreous body, the peak compressive stresses were 0.5-0.6 kPa and the peak tensile stresses were *ca.* 0.2 kPa, smaller than those of 1.0% and 0.5% agar gels. On the other hand, all model materials responded similarly in the simulations of accidental falls (Fig. 7).

In contrast to the instantaneous and linear impact due to falling, shaking followed rather complex trajectory. That less tensile stress was observed in eyeball model containing water subjected to abusive

shaking suggests that the physical constraints due to agar gel plays an important role in RH in SBS / AHT. These results suggest that infant vitreous body, which has much ingredient of gel¹², may lead to severer RH through shaking events because larger tensile stresses may be applied to the retina than that of adults, which has less ingredient of gel.

3.4. Effects of machine-controlled oscillation on the eyeball model

Fig. 8 shows a typical portion of measurements with the eyeball model containing 0.5% agar gel subjected to reproducible sinusoidal shaking generated with an oscillation machine. Spikes seen in the acceleration curve (Fig. 8B) were probably caused by sudden shifts of oil pressure in the actuator of the oscillation machine. Fortunately, these spikes did not result in any visible noise in the displacement (Fig. 8A). The sinusoidal curve fitted by the least squares method was used for the estimation of the stress at the posterior pole (Fig. 8C) because we regarded these spikes negligible. Similar measurements were also carried out with the eyeball model containing 1.0% agar gel and water. Fig. 9 shows the effects of different model materials when the eyeball models were subjected to sinusoidal shaking. Fig. 10 shows measurements with the eyeball model containing 0.5% agar gel subjected to rectangular pulse movements generated with the oscillation machine, simulating impacts. Similar measurements were also carried out with the eyeball model containing 1.0% agar gel and water. Fig. 11 shows the effects of model materials with the acceleration of impacts.

The stress applied by shaking and impacting using the oscillation machine was similar (Figs. 9 and 11), which is inconsistent with the corresponding results using the dummy doll (Figs. 6 and 7). This is probably due to that the machine-controlled oscillation was simple and uniaxial, while the simulation using the dummy doll resulted in a rather complex trajectory. The gradient of the stress along the longitude in the eyeball model containing water was more gradual than those containing 1.0% and 0.5% agar gels. The difference of the gradient may be the cause of the difference seen in the tensile stress in Fig. 6.

4. Discussion

Duhaime et al.⁸ compared experimental results using a dummy doll with a tolerance limit deduced from animal experiments, and stated that shaking alone is unlikely to cause severe SBS / AHT. Cory and Jones¹⁷ questioned this statement through a parametric study using an adjustable dummy doll and an updated tolerance limit. However, these approaches have a common inherent difficulty on interpretation because of the uncertainty of the tolerance limit, which mainly arises from the complexity of the mechanism leading to the outcome symptoms and the anatomical divergence of animal models from human infants.

Thus, it may be useful to consider from a different perspective. We aimed to estimate a physical parameter by using a simple model, instead of inferring outcome symptoms from a realistic model. The major step forward made in this study is the estimation of the stress applied on the retinal tissue. The

maximal stress observed in shaking, 1 kPa, is approximately equivalent to the gravitational traction by a mass of 10 g applied to an area of 1 cm², while an order of magnitude greater stress was observed in falling. This physical parameter provides a concrete measure on the mechanical state of the retinal tissue.

One may argue, however, that our model is an oversimplification. For example, the eyeball model was rigidly attached to the head of the dummy doll made of plastic, which may be considered unrealistic because a real eyeball is surrounded by fat and soft tissue in the orbit and has no direct rigid attachment to the skull. While the absence of this soft cushion around the eyeball might significantly exaggerate the stress in some cases of falling, its effect on shaking stress would not be a prominent one. The structure of the neck of our dummy doll, plastic head sewed to body made of cloth, may also be considered unrealistic, but at least the acceleration experienced by the head of the dummy doll (Figs. 2-4) roughly agreed with those of a previous study⁸. The method of the estimation of the Young's moduli of the model of the vitreous body may also be criticized, but it was shown to have minor effect on the results (Figs. 6 and 7). Analogy from the parametric study by Cory and Jones¹⁷ suggests that we should anticipate as much as five-times difference in the estimations, due to that we were not able to properly model these details.

Considering the potentially wide variety in the situations of abusive shaking and accidental falls, in addition to the uncertainties discussed in the previous paragraph, it might not be appropriate to assume any kind of tolerance limit and to deduce outcome symptoms in this study. We would rather confine the discussion to the comparison of the normal stress between the situations of abusive shaking and accidental falls, both of which measured using the same model.

Table 4 compares violent shaking with accidental falls, simulated with the eyeball model containing 1.0% and 0.5% agar gels. Abusive shaking and accidental falls are clearly different in the intensity and the duration of the stresses; abusive shaking are with far less intensity but far longer duration, compared to accidental falls. Obviously, both intensity and duration of stress applied on the retina would have major effect on RH. To compare the effects of abusive shaking and accidental falls, which are very different phenomena with each other, the most straightforward common measure would be the time integral of stress. In the model containing 0.5% agar gel, the time integral of the stress due to a single cycle of shaking was 107 Pa-s, much larger than that of a single event of fall, 60 to 73 Pa-s. Taking into account that abusive shaking has multiple cycles, the time integral of the stress can be even larger. Although Cory and Jones¹⁷ reported that their volunteer adults felt quite difficult to shake more than ten seconds, stress integrated for few seconds of shake readily surpasses that of single event of fall.

Admitted that time integral of stress is a relevant measure, why RH is frequent in SBS / AHT but rare in accidental falls would be clearly explained. Time integral of stress might account for the cumulative effect of shaking or multiple impacts suggested by Cory and Jones¹⁷. Although whether these conditions do lead to the observed symptoms of RH awaits validation with animal experiments, this study offers for such future experiments a possibility to consider mechanical stress applied on the retinal tissue separately

from the divergence of anatomical configurations and proportions of organs.

5. Conclusions

The mechanism of SBS / AHT was experimentally studied using a dummy doll equipped with an eyeball model. The possibly worst-case scenario of abusive shaking was explored, and was compared to that of accidental falls. The normal stresses applied on the retina during abusive shaking and accidental falls were estimated and compared. We suggest the time integrals of normal stress applied on the retina, 107 Pa·s per cycle of shaking and 60 to 73 Pa·s for a single event of fall, as a relevant parameter affecting RH in SBS / AHT.

Conflict of Interest Statement

The authors declare no conflict of interest.

Acknowledgments

This study is a part of a project entitled "Protecting Children from Crime" supported by the Research Institute of Science and Technology for Society (RISTEX), Japan Science and Technology Agency (JST). We would like to thank Dr. Fujiko Yamada at Child Maltreatment Prevention Network for her provision of the dummy doll. We also would like to thank Dr. Yuri Nakayama at Division of Ophthalmology, National Center for Child Health and Development for the advices based on her surgical experience. We are also grateful to Mr. Gen Tamaoki at Department of Mechanical Engineering, Tokyo Metropolitan University for the permission to use an oscillation machine and for the support on using it.

References

- [1] Hadley, M.N., Sonntag, V.K.H., ReKate, H.L., Murphy, A.. The infant whiplash-shake injury syndrome: A clinical and pathological study. *Neurosurgery* 1989;24(4):536–540.
- [2] King, W.J., MacKay, M., Sirnack, A., The Canadian Shaken Baby Study Group, . Shaken baby syndrome in Canada: Clinical characteristics and outcomes of hospital cases. *Canadian Medical Association Journal* 2003;168(2):155–159.
- [3] Atwal, G.S., Ruttly, G.N., Carter, N., Green, M.A.. Bruising in non-accidental head injured children; a retrospective study of the prevalence, distribution and pathological associations in 24 cases. *Forensic Science International* 1998;96(2):215–230. doi:10.1016/S0379-0738(98)00126-1.
- [4] Sturm, V., Landau, K., Menke, M.N.. Optical coherence tomography findings in shaken baby syndrome. *American Journal of Ophthalmology* 2008;146(3):363–368. doi:10.1016/j.ajo.2008.04.023.
- [5] Bechtel, K., Stoessel, K., Leventhal, J.M., Ogle, E., Teague, B., Laviertes, S., et al. Characteristics that distinguish accidental from abusive injury in hospitalized young children with head trauma. *Pediatrics* 2004;114(1):165–168. doi:10.1542/peds.114.1.165.

- [6] Trenchs, V., Curcoy, A.I., Morales, M., Serra, A., Navarro, R., Pou, J.. Retinal haemorrhages in head trauma resulting from falls: Differential diagnosis with non-accidental trauma in patients younger than 2 years of age. *Child's Nervous System* 2008;24(7):815–820. doi:10.1007/s00381-008-0583-y.
- [7] Balazs, E.A., Denlinger, J.L.. Aging changes in the vitreous. In: Sekuler, R., Dismukes, K., Kline, D., National Research Council (U.S.). Committee on Vision, , editors. *Aging and Human Visual Function*; vol. 2 of *Modern Aging Research*. New York: A. R. Liss; 1982, p. 45–47.
- [8] Duhaime, A.C., Gennarelli, T.A., Thibault, L.E., Bruce, D.A., Margulies, S.S., Wisner, R.. The shaken baby syndrome. *Journal of Neurosurgery* 1987;66(3):409–415.
- [9] Wygnanski-Jaffe, T., Morad, Y., Levin, A.V.. Pathology of retinal hemorrhage in abusive head trauma. *Forensic Science, Medicine, and Pathology* 2009;5(4):291–297.
- [10] Hans, S.A., Bawab, S.Y., Woodhouse, M.L.. A finite element infant eye model to investigate retinal forces in shaken baby syndrome. *Graefe's Archive for Clinical and Experimental Ophthalmology* 2009;247(4):561–571. doi:10.1007/s00417-008-0994-1.
- [11] Rangarajan, N., Kamalakkannan, S.B., Hasija, V., Shams, T., Jenny, C., Serbanescu, I., et al. Finite element model of ocular injury in abusive head trauma. *Journal of AAPOS* 2009;13(4):364–369. doi:10.1016/j.jaaapos.2008.11.006.
- [12] Sebag, J.. Macromolecular structure of the corpus vitreus. *Progress in Polymer Science* 1998;23(3):415–446. doi:10.1016/S0079-6700(97)00035-X.
- [13] Zimmerman, R.L.. In vivo measurements of the viscoelasticity of the human vitreous humor. *Biophysical Journal* 1980;29(3):539–544. doi:10.1016/S0006-3495(80)85152-6.
- [14] Lee, B., Litt, M., Buchsbaum, G.. Rheology of the vitreous body. part I: Viscoelasticity of human vitreous. *Biorheology* 1992;29(5–6):521–533.
- [15] Piccirelli, M., Bergamin, O., Landau, K., Boesiger, P., Luechinger, R.. Vitreous deformation during eye movement. *NMR in Biomedicine* 2012;25(1):59–66. doi:10.1002/nbm.1713.
- [16] Kobayashi, Y., Yamada, K., Ohba, S., Nishina, S., Okuyama, M., Azuma, N.. Ocular manifestations and prognosis of shaken baby syndrome in two Japanese children's hospitals. *Japanese Journal of Ophthalmology* 2009;53(4):384–388. doi:10.1007/s10384-009-0681-8.
- [17] Cory, C.Z., Jones, M.D.. Can shaking alone cause fatal brain injury? a biomechanical assessment of the Duhaime shaken baby syndrome model. *Medicine, Science and the Law* 2003;43(4):317–333. doi:10.1258/rsmmsl.43.4.317.

Table 1: Characteristics of the imitate perpetrators.

	Sex	Age	Height (cm)	Experience of holding or bringing up a baby
a	female	21	173	no experience
b	female	20	162	holding, 2 years old
c	female	20	157	holding, 1 year old
d	female	36	169	bringing up, from the birth to 10 years old
e	female	20	155	holding, from the birth to 5 years old
f	male	24	166	no experience

Table 2: Characteristics of violent shaking by each imitate perpetrator without any instructions. The eyeball model contained 1.0% agar gel as a model of the vitreous body.

	Frequency of the acceleration-deceleration history experienced by the head of the dummy doll (Hz)	Peak intensities of the acceleration experienced by the head of the dummy doll (m/s^2)		Peak intensities of the stress at the posterior pole (kPa)		Number of shakes
		Posterior direction	Anterior direction	Compressive	Tensile	
a	2.70 ± 0.47	80.9 ± 28.8	-29.0 ± 17.2	-1.08 ± 0.44	0.44 ± 0.20	37
b*	1.83 ± 0.13	36.5 ± 7.5	-41.9 ± 8.3	-0.55 ± 0.09	0.64 ± 0.07	18
c	3.21 ± 0.28	32.1 ± 8.8	-34.1 ± 7.0	-0.58 ± 0.09	0.50 ± 0.10	46
d	2.58 ± 0.95	40.9 ± 12.9	-42.9 ± 15.9	-0.63 ± 0.15	0.55 ± 0.19	39
e	1.95 ± 0.22	38.0 ± 5.6	-39.1 ± 11.5	-0.56 ± 0.08	0.52 ± 0.12	27
f**	–	–	–	–	–	–
average	2.45 ± 0.57	45.7 ± 20.0	-37.4 ± 5.8	-0.68 ± 0.23	0.53 ± 0.08	

*b shook the dummy doll vertically, while the others shook horizontally.

**f is the person who explored the modes of shaking in Figs. 2-4

Table 3: Characteristics of violent shaking by each imitate perpetrator instructed to reproduce the mode of shaking shown in Fig. 4. The eyeball model contained 1.0% agar gel as a model of the vitreous body.

	Frequency of the acceleration-deceleration history experienced by the head of the dummy doll (Hz)	Peak intensities of the acceleration experienced by the head of the dummy doll (m/s^2)		Peak intensities of the stress at the posterior pole (kPa)		Number of shakes
		Posterior direction	Anterior direction	Compressive	Tensile	
a	1.51 ± 0.20	70.1 ± 20.0	-58.1 ± 9.0	-1.15 ± 0.74	0.74 ± 0.17	21
b	1.55 ± 0.16	39.5 ± 8.7	-33.4 ± 7.0	-0.59 ± 0.13	0.54 ± 0.07	15
c	1.60 ± 0.28	44.5 ± 17.5	-39.5 ± 10.3	-0.66 ± 0.18	0.55 ± 0.13	24
d	1.48 ± 0.16	61.2 ± 11.9	-36.5 ± 4.9	-0.81 ± 0.18	0.61 ± 0.12	39
e	1.81 ± 0.11	64.2 ± 9.8	-40.1 ± 7.7	-0.83 ± 0.16	0.57 ± 0.11	27
f	2.15 ± 0.11	79.7 ± 15.1	-45.1 ± 4.3	-1.05 ± 0.24	0.68 ± 0.12	31
average	1.68 ± 0.26	59.9 ± 15.3	-42.1 ± 8.8	-0.85 ± 0.22	0.62 ± 0.08	–

Table 4: Comparing violent shaking with accidental falls, simulated with the eyeball model containing 1.0% or 0.5% agar gel.

Conditions	Time integral of the stress (Pa·s)		Maximum stress (kPa)		Duration of the stress (ms)	
	1.0%	0.5%	1.0%	0.5%	1.0%	0.5%
	Single cycle of shaking with a mode shown in Fig. 4	191	107	1.0	0.9	325
50-cm fall to a cushion	56	60	3.0	3.4	74	69
100-cm fall to a cushion	87	73	12.7	8.6	38	36
50-cm fall to a hard floor	80	70	14.2	13.1	13	21

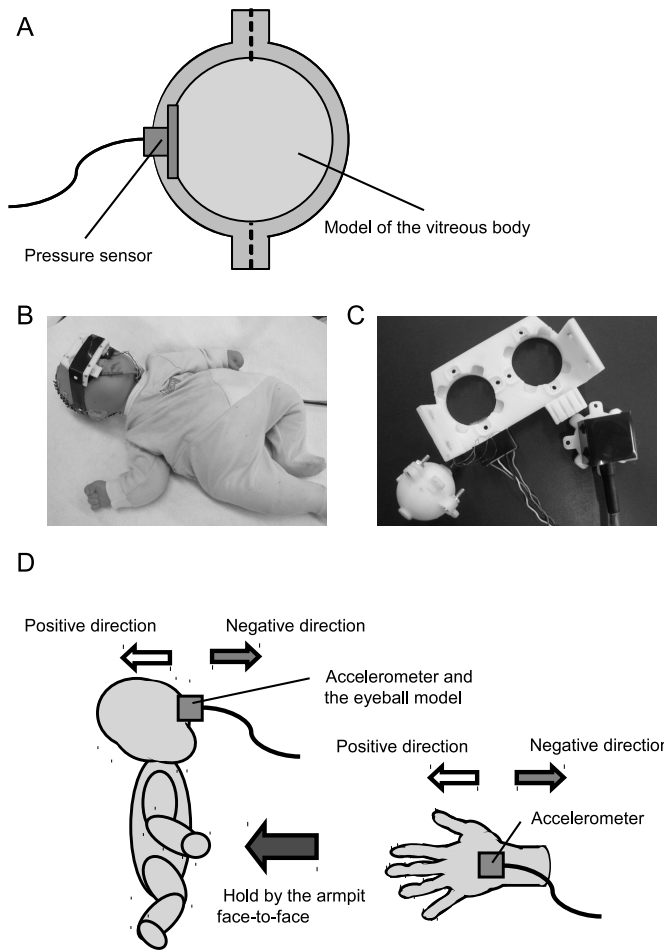


Figure 1: Experimental setup to simulate abusive shaking. The plastic casing of the eyeball model contained either agar gel or water as a model of the vitreous body (A). A pressure sensor was placed on the inside wall of the casing. A dummy doll simulating an one-month-old infant was prepared (B). The eyeball model (bottom left) and an accelerometer (bottom right) were fixed via an attachment (top) to the head of the doll (C). The coordinate system of the accelerometers in the simulation of violent shaking is shown (D). An imitate perpetrator held the dummy doll by the armpits face-to-face. An accelerometer was attached to either of the hands of the imitate perpetrator, the positive direction of the coordinate system of which corresponded to the direction of the stroke moving away from the body of the imitate perpetrator. Another accelerometer was attached to the head of the dummy doll parallel to the sagittal axis, the positive direction of the coordinate system of which corresponded to the posterior direction of the head of the dummy doll.

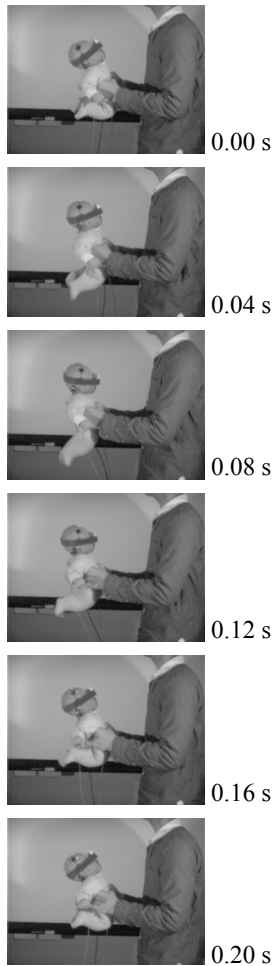
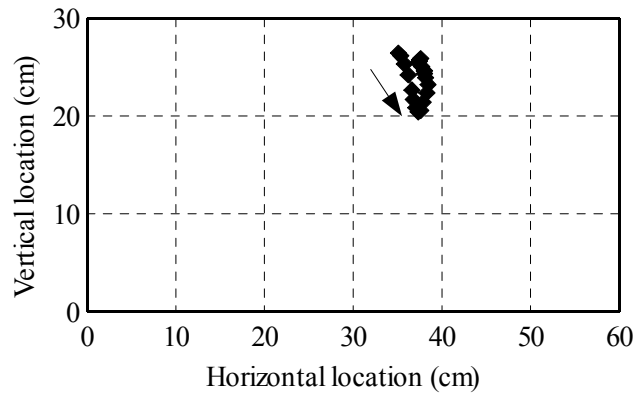
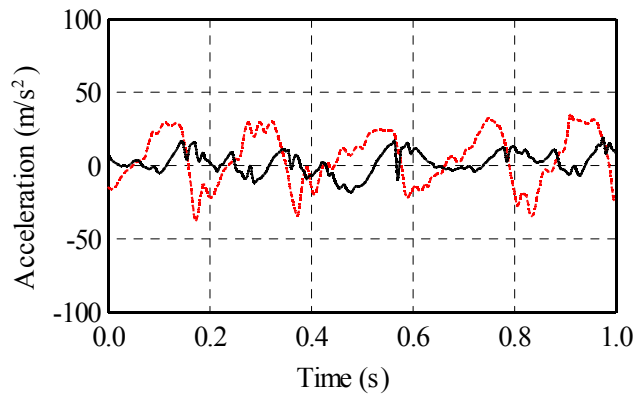
A**B****C**

Figure 2: Fast shaking with the fore arms. (A) shows continuous pictures of a typical single cycle of the violent shaking. (B) shows the locus of the eyeball model fixed on the head of the dummy doll along a typical single cycle of the shaking. The arrow shows the direction of the movement. The location of the eyeball model was manually extracted from the moving picture every 0.01 s. The location of the body of the imitate perpetrator was at about 70 cm. (C) shows a typical portion of time history of the acceleration. The solid curve shows the acceleration experienced by the head of the dummy doll. The dotted curve shows that recorded on the hand of the imitate perpetrator.

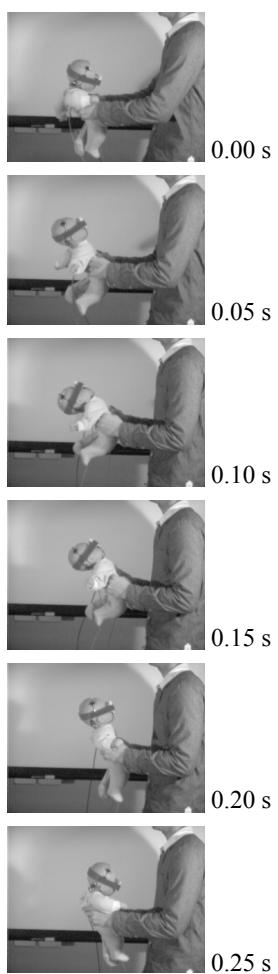
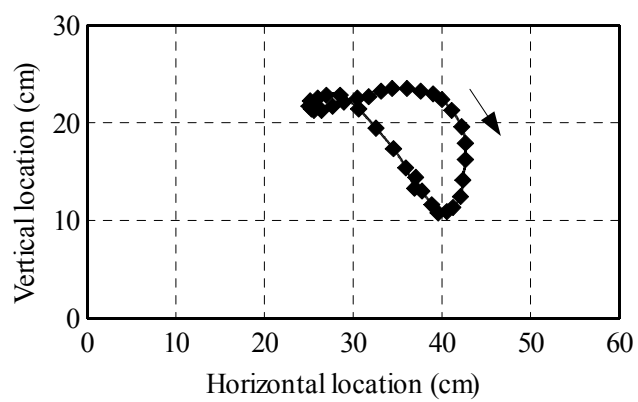
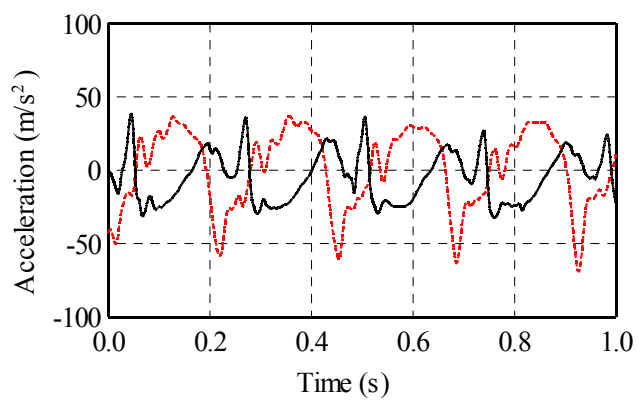
A**B****C**

Figure 3: Fast shaking with the whole arms. Details are as in Fig. 2.

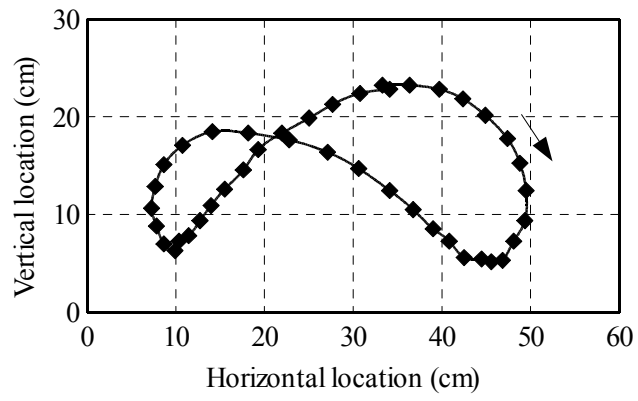
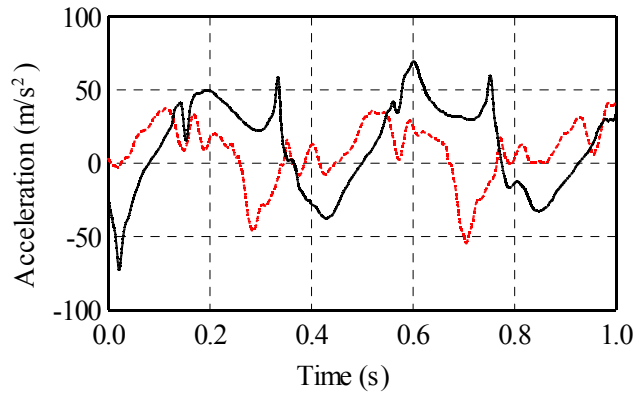
A**B****C**

Figure 4: Synchronized shaking with the whole arms. Details are as in Fig. 2.

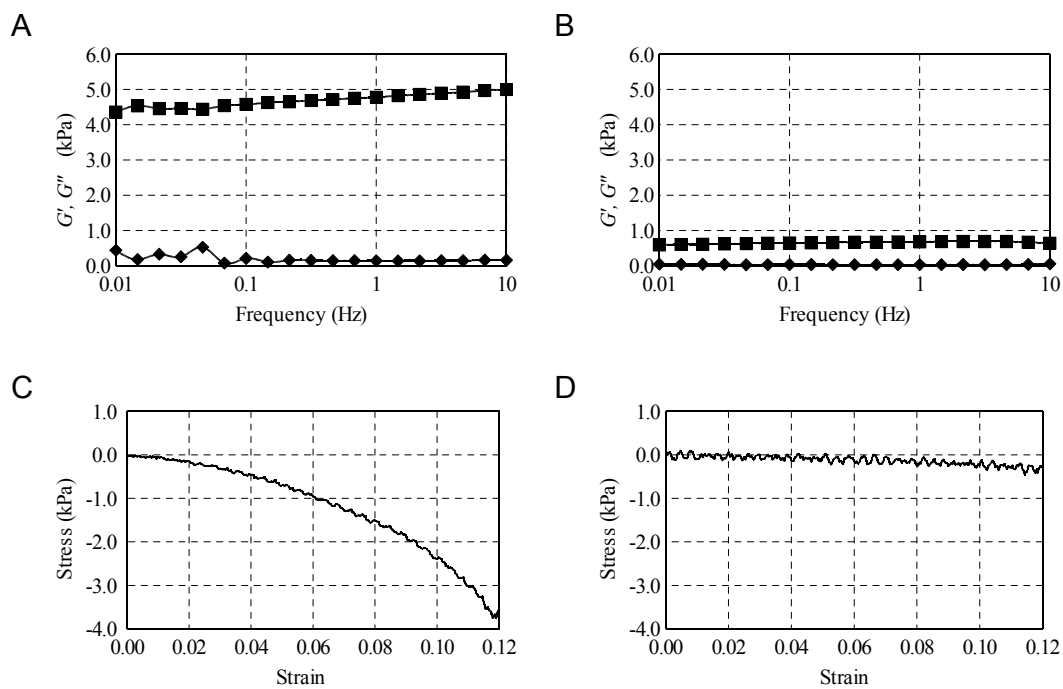


Figure 5: Mechanical properties of the agar gels. (A) and (B) show the viscoelasticity of 1.0% and 0.5% agar gels, respectively. The elastic and viscous properties were measured with a rotational rheometer by frequency sweep at the shearing stress of 10 Pa. Squares show the storage modulus G' and diamonds show the loss modulus G'' . (C) and (D) show stress-strain curves of 1.0% and 0.5% agar gels, respectively. The average of 10 measurements with a compressive velocity of 10 mm/s are shown.

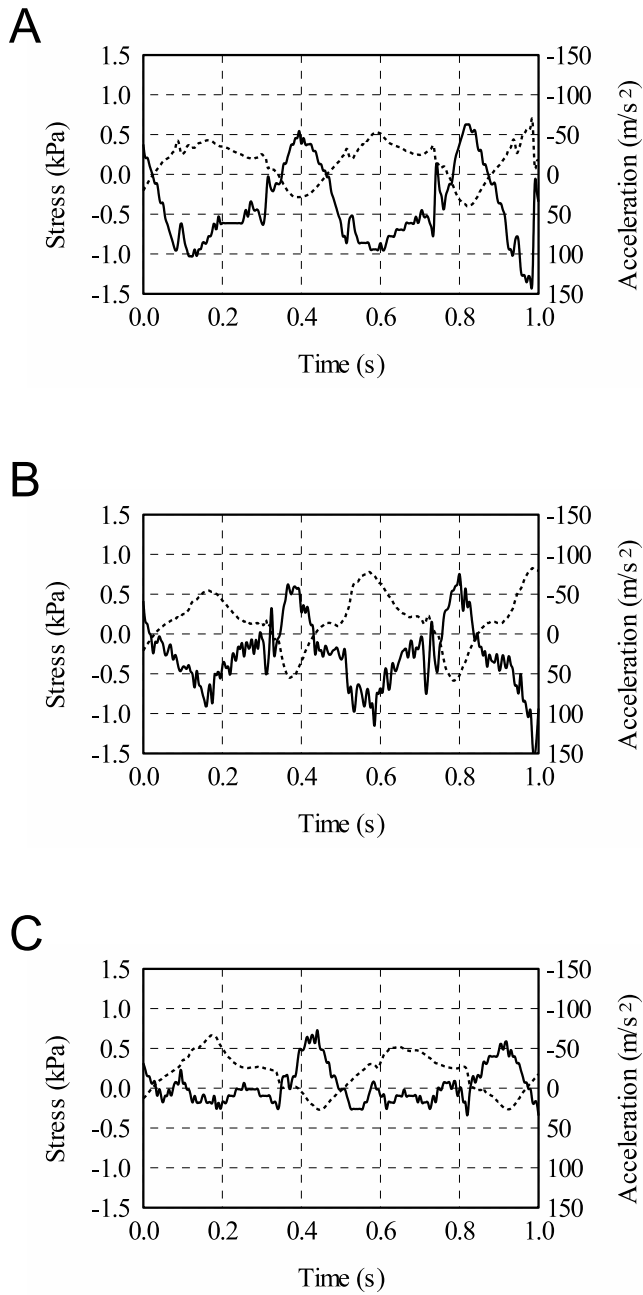


Figure 6: Effects of model materials of the vitreous body on the stress applied to the retina at the posterior pole due to the mode of shaking shown in Fig. 4. Solid curves (left ordinate) show typical portions of the stress histories recorded with a pressure sensor set inside the eyeball model at the posterior pole. Dotted curves (right ordinate, note the inverted scale) show the corresponding acceleration histories experienced by the head of the dummy doll, on which the eyeball model was fixed. (A), (B) and (C) show those with the eyeball model containing 1.0% and 0.5% agar gels and water, respectively.

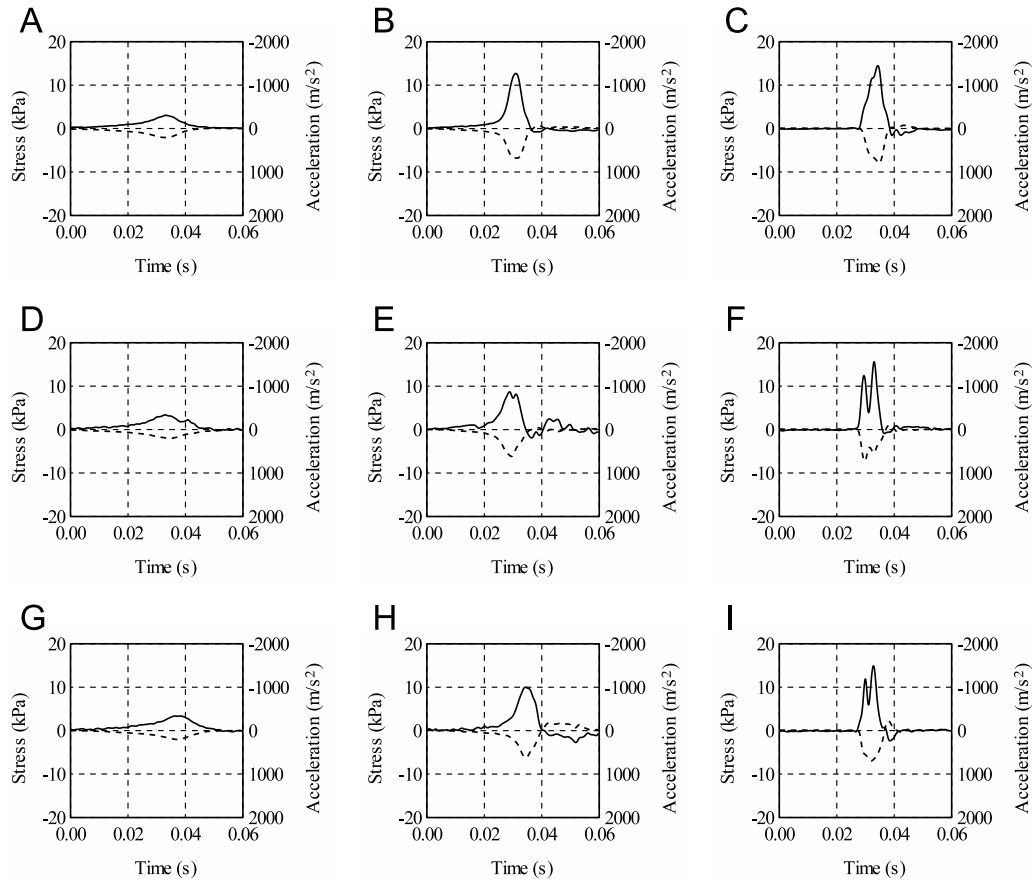


Figure 7: Effects of model materials of the vitreous body on the stress applied to the retina at the posterior pole in simulations of accidental falls. Solid curves (left ordinate) show the stress histories recorded with a pressure sensor set inside the eyeball model at the posterior pole. Dotted curves (right ordinate, note the inverted scale) show the acceleration histories experienced by the head of the dummy doll, on which the eyeball model was fixed. The eyeball model contained 1.0% agar gel in (A), (B) and (C), 0.5% agar gel in (D), (E) and (F) and water in (G), (H) and (I), respectively. (A), (D) and (G) show 50-cm falls to a cushion, (B), (E) and (H) show 100-cm falls to a cushion and (C), (F) and (I) show 50-cm falls to a hard floor, respectively.

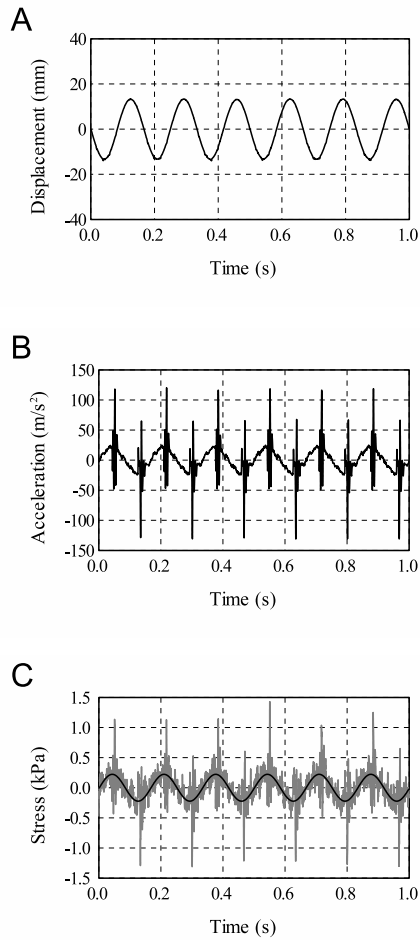


Figure 8: Eyeball model subjected to reproducible sinusoidal shaking generated with an oscillation machine. The eyeball model containing 0.5% agar gel as a model of the vitreous body was sinusoidally shaken with the frequency of 6.0 Hz and the stroke of 30 mm. (A), (B) and (C) show the displacement of the eyeball model, the acceleration experienced by the eyeball model and the stress at the posterior pole, respectively. The anterior direction of the eyeball model placed on the oscillation machine corresponds to the positive direction of the displacement in (A). The anterior direction of the acceleration corresponds to the positive direction in (B). The black curve in (C) shows the sinusoidal curve fitted to the original data, the gray curve, by the least squares method.

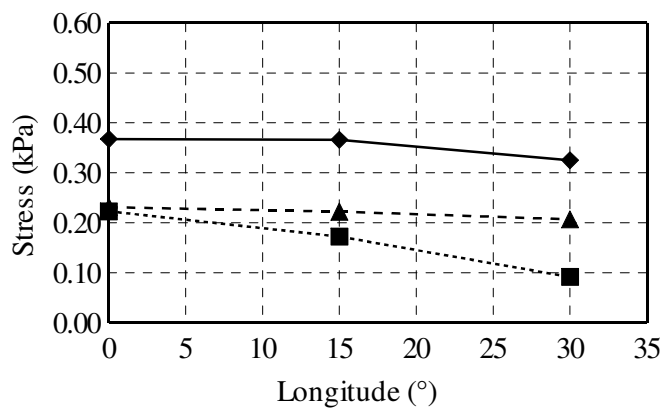


Figure 9: Peak stress distribution due to sinusoidal acceleration-deceleration. The stress normal to the retinal plane was plotted along the longitudinal location with respect to the axis of the motion of the oscillation. The set of data were recorded by altering the angle of the eyeball model in the experimental setup. Diamonds, squares and triangles show the data of the eyeball model containing 1.0%, 0.5% agar gels and water as a model of the vitreous body, respectively. The plots are based on data similar to that shown in Fig. 8.

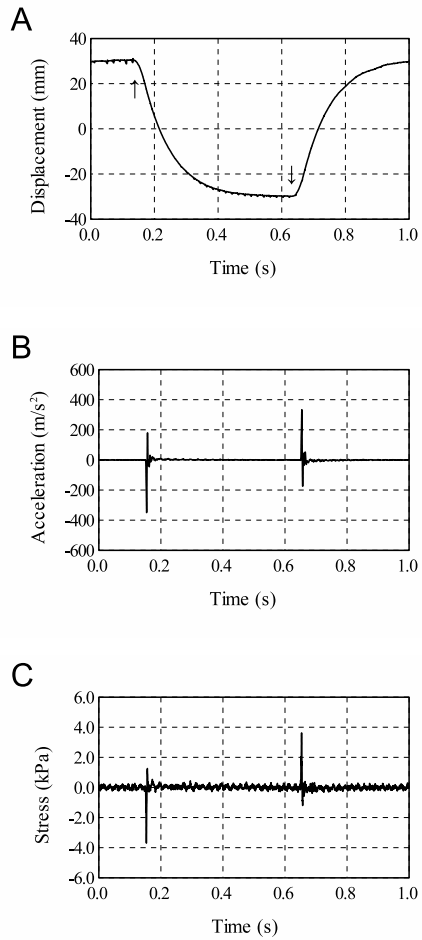


Figure 10: Eyeball model subjected to rectangular pulse movements generated with an oscillation machine. The eyeball model containing 0.5% agar gel as a model of the vitreous body was subjected to rectangular pulse movements simulating impacts with the stroke of 50 mm. (A), (B) and (C) show the displacement of the eyeball model, the acceleration experienced by the eyeball model and the stress at the posterior pole, respectively. Downward and upward arrows in (A) show rectangular pulse movement with positive and negative displacement, respectively. The coordinate system was as in Fig. 8.

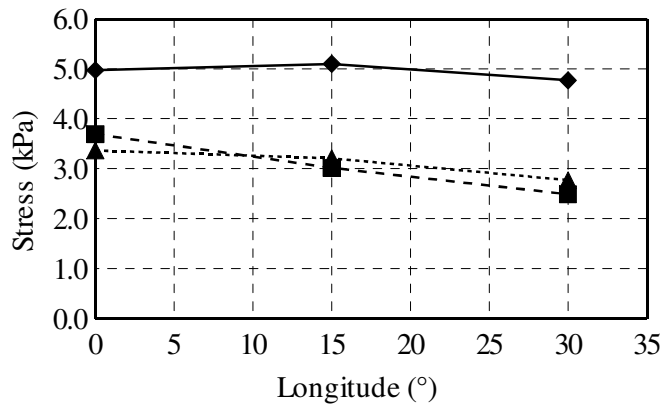


Figure 11: Peak stress distribution due to the acceleration of impacts. Details are as in Fig. 9. The plots are based on data similar to that shown in Fig. 10.